Detailed Mechanism for AmtB Conducting NH_4^+/NH_3: Molecular Dynamics Simulations

Huaiyu Yang, Yechun Xu, Weiliang Zhu, Kaixian Chen, and Hualiang Jiang
Drug Discovery and Design Center, State Key Laboratory of Drug Research, Shanghai Institute of Materia Medica, Shanghai Institutes for Biological Science and Graduate School, Chinese Academy of Sciences, Shanghai 201203, China

ABSTRACT The mechanism by which the ammonium transporter, AmtB, conducts NH_4^+/NH_3 into the cytoplasm was investigated using conventional molecular dynamics (MD) simulations. These simulations revealed that the neutral molecule, NH_3, passes automatically through the channel upon its arrival at the Am2 site and that the function of the channel as a one-way valve for passage of NH_3 is not determined by the cytoplasmic exit gate but, rather, by the periplasmic entrance gate of the channel. The NH_3, produced by deprotonation of NH_4^+ at the entrance gate, is spontaneously conveyed to the central region of the channel via a hydrogen-bond network comprising His-168, His-318, Tyr-32, and the NH_3 molecule. Finally, the NH_3 molecule exits the channel through the exit gate formed by Phe-31, Ile-266, Val-314, and His-318. In addition, Ser-263 is shown to play a critical role in the final stages, acting as a pivoting arm to shunt the NH_3 molecule from the cytoplasmic exit gate of the channel out into the cytoplasm. This finding is further supported by another simulation which shows that NH_3 fails to be translocated through the channel formed by the Ser-263–Ala mutation. Thus, this study casts new insights on the mechanism of AmtB-mediated passage of NH_3 across cellular membranes.

INTRODUCTION

The transport of ammonium across cellular membranes is critical for the acquisition and metabolism of nitrogen in a diverse range of organisms from bacteria to man (1,2). The ammonia/ammonium transporter protein family includes the ammonium transporters (Amts) and methylamine permeases (MEPs), and these proteins are typically 400–500 amino acids in length (3–5).

Ammonia/ammonium conductance facilitated by the Amt/MEP family of proteins is concentration dependent. At high extracellular ammonium concentrations, AmtB transporter activity is inhibited through complex formation with the regulatory GlnK protein, a member of the P_{II} protein family (2,6,7). Under these conditions, passive membrane permeation of NH_3 may be sufficient to promote cell growth (2). However, at low ammonium concentrations, GlnK does not interact with AmtB, and the function of AmtB for ammonia/ammonium translocation is activated. At the outset of our studies, the widely accepted view was that the target molecule in ammonia/ammonium translocation was NH_4^+. However, other experiments suggested that NH_3 could be the entity that is translocated (8,9). A series of studies investigating substrate specificity has been performed (2,10) and discordant conclusions have been drawn. Some studies indicate that the Amt/MEP family of proteins mediate the uptake of the analog, (methyl)ammonium, into the cell depending on the membrane potential and pH values, prompting the notion that these proteins are involved in the movement of NH_4^+ from the periplasm into the cytoplasm (2,10). In contrast, other studies show that AmtB conduct NH_3 bidirectionally (8,9). Cellular studies conducted by Soupene et al. reveal that AmtB can facilitate the passage of NH_3 molecules into the cytoplasm.

The crystal structures of *Escherichia coli* AmtB show that it is a channel that spans the cellular membrane 11 times (Fig. 1 *A*) (11,12). On its periplasmic side (referred to as the top hereafter, Fig. 1 *A*), the channel is sheltered by Phe-107 and Phe-215, whereas the cytoplasmic side (referred to as the bottom) of the channel is blocked by Phe-31. The presence of an electron density peak outside the entrance gate in the crystal structure indicates that this could be the NH_4^+ binding site (Am1 site in Fig. 1 *A*) (11). Cation-π interactions with Phe-103, Phe-107, and Trp-148, as well as hydrogen-bond interactions with Ser-219, were postulated to be molecular determinants of NH_4^+ binding in AmtB (13). Furthermore, there are three weak peaks (Am2–Am4 sites in Fig. 1 *A*) inside the channel which are presumed to be three NH_3 molecules (11). On the other hand, two significant studies challenged the view that NH_3 is observed in the center of the channel (12,14). Two histidine residues, His-168 and His-318, located in the middle of the channel, are linked via a hydrogen bond formed in two possible ways: between deprotonated His-168 N^{δ} and the H of His-318 $N^{\delta}H$ (Fig. 1 *B*) or between deprotonated His-318 N^{δ} and the H of His-168 $N^{\delta}H$ (Fig. 1 *C*). Hence, there are two plausible states of the His-168-His-318 system: 1), hydrogen atoms are added to N^{ε} of His-168 and N^{δ} of His-318 (referred to as the first protonation state); or 2), hydrogen atoms are added to N^{δ} of His-168 and N^{ε} of His-318 (referred to as the second protonation state). Khademi et al. proposed that unprotonated His-168 N^{δ} and His-318 $N^{\delta}H$ are held

Submitted May 30, 2006, and accepted for publication October 16, 2006.

Address reprint requests to Weiliang Zhu or Hualiang Jiang, Drug Discovery and Design Center, Shanghai Institute of Materia Medica, 555 Zuchongzhi Road, Shanghai 201203, China. Tel.: 86-21-5080-5020; Fax: 86-21-5080-7088; E-mail: wlzhu@mail.shcnc.ac.cn; hljiang@mail.shcnc.ac.cn.

0006-3495/07/02/877/09 $2.00

doi: 10.1529/biophysj.106.090191

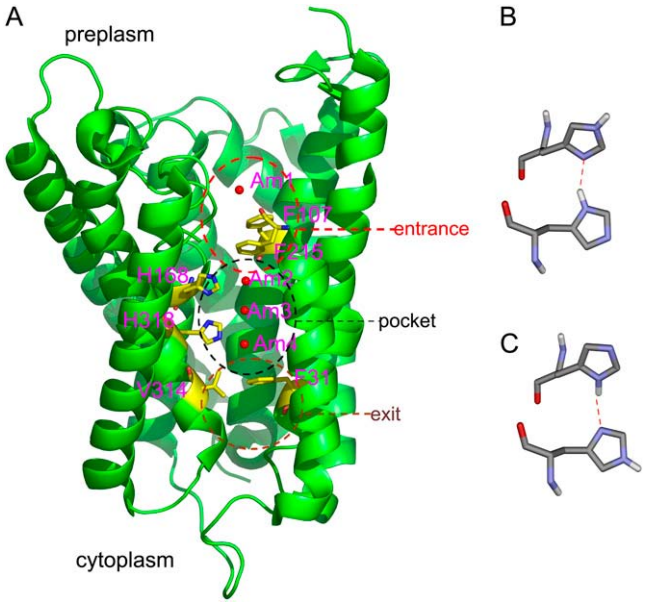

FIGURE 1 (*A*) Structure of AmtB (1U7G.pdb). Residues 214–272 are not shown for clarity. Some important residues are shown in stick representation. NH_4^+ or NH_3 are variably put at the four sites (Am1–Am4, *red spheres*) in simulations. Entrance region, hydrophobic region, and exit region are simply indexed by red, black, and brown circles, respectively. (*B*) The first state of the neutral His-168-His-318 system where the hydrogen atoms are added to N^{ε} of His-168 and N^{δ} of His-318. (*C*) The second state of the neutral His-168-His-318 system where the hydrogen atoms are added to N^{δ} of His-168 and N^{ε} of His-318.

rigidly by a hydrogen bond, and the C=O of Leu-269 forms another hydrogen bond with the H of His-318 $N^{\delta}H$ (11).

Although mechanistic information on the channel is available, further insights into the mode of ammonia/ammonium conductance at the atomic level has yet to be elucidated, especially the dynamic process of translocation. In addition, the exact site where NH_4^+ releases H^+ remains unknown. Deprotonation may take place either outside the channel or inside the channel, probably at the Am1 or Am2 site. Furthermore, it is also difficult to clarify the effects of the two protonation states of His-168 and His-318 on ammonia/ammonium conductance using crystallographic and biochemical methods. In addition, two different conformational states of the cytoplasmic exit of the channel have been observed in two different crystal forms (12). It is compelling to ask, then, what is the exit gating mechanism of the channel responsible for transport of small molecules? Does the conformational structure of the channel change from one form to another during NH_3 translocation?

Molecular dynamics (MD) simulations have been used to study membrane permeation of small molecules, a process that resembles that of ammonia translocation across membranes. For example, Groot et al. studied water permeation through aquaporin (15). Here, we report new insights into the mechanistic mode of ammonia/ammonium conductance through AmtB derived from a series of long time MD simulations on the systems where AmtB/NH_3, AmtB/NH_4^+ complexes were embedded in a water-solvated dipalmitoyl phosphatidylcholine (DPPC) bilayer. For the first time, the simulations show that NH_3 molecules can pass through AmtB spontaneously in both states of His-168-His-318 protonation via an exit gate facilitated by Ser-263.

METHODS

Materials

The coordinates of AmtB were obtained from the crystal structure determined at pH 6.5 (14) (Protein Data Bank (PDB) entry 1U7G). Mutations (F68S, S126P, and K255L) were modified by using the molecular modeling software Sybyl 6.8 (Tripos, St. Louis, MO). The protein was fitted into the DPPC bilayer with 309 lipids (15,450 atoms) to generate a suitable membrane system (Fig. 2). Coordinates for crystal water molecules near the entrance gate were kept and hydrogen atoms were added using the software Sybyl 6.8. Then the protein/DPPC systems were solvated in a bath of 16,661 SPC water molecules (16). Water molecules in the region which are occupied by a β-octyl glucoside molecule in the crystal structure were deleted. Thereafter, NH_3 molecules were variably added to three sites (Am2, Am3,

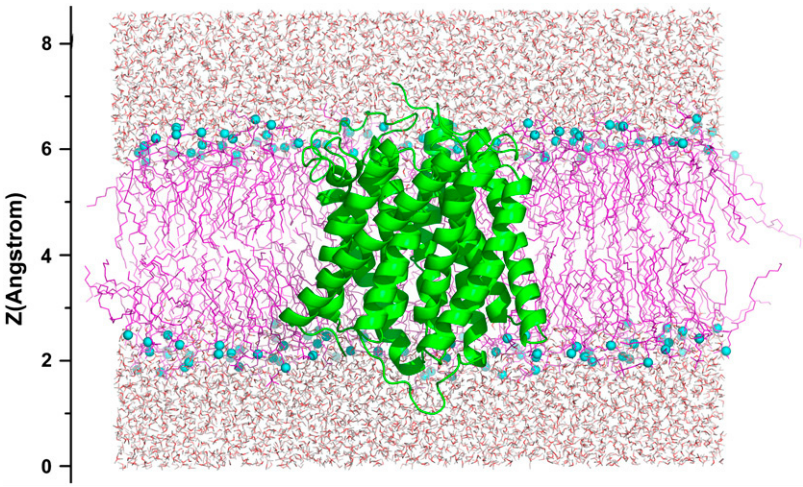

FIGURE 2 Side view of the simulation system. The AmtB protein is shown as a green ribbon, phosphate atoms are drawn as cyan spheres, the other atoms of the lipid are represented as magenta lines, and water molecules are displayed as red and white sticks. The front half of the bilayer is not shown for the sake of clarity.

TABLE 1 Detailed information for MD simulations

Trajectory	Am2	Am3	Am4	His-168	His-318	Time (ns)
A1	NH_3	NH_3	NH_3	$N^{\varepsilon}H$	$N^{\delta}H$	8
A2	NH_3	NH_3	NH_3	$N^{\delta}H$	$N^{\varepsilon}H$	10
B*	NH_3	NH_3	NH_3	$N^{\varepsilon}H$	$N^{\delta}H$	20
C1	NH_4^+	–	–	$N^{\delta}H$	$N^{\varepsilon}H$	2
C2	NH_4^+	–	–	$N^{\delta}H$	$N^{\varepsilon}H$	2

*Ser-263 was mutated to alanine.

and Am4 in Fig. 1 *A*) as shown in Table 1. To perform the modeling under simulated physiological conditions, Na^+/Cl^- ions were then added to neutralize the modeled system.

Details of these MD simulations are listed in Table 1. In simulations A1, A2, and B, three NH_3 molecules were placed at the Am2–Am4 sites, respectively, whereas in simulations C1 and C2, only one NH_4^+ was placed at the Am2 site. Simulations A1 and B adopted the first protonation state for His-168-His-318 involving addition of hydrogen atoms to the N^{ε} and N^{δ} atoms of His-168 and His-318, respectively (Fig. 1 *B*), whereas the other simulations used the second state of protonation for His-168-His-318 whereby the N^{δ} atom of His-168 and the N^{ε} atom of His-318 were protonated (Fig. 1 *C*). Simulation B on the mutant Ser-263-Ala was performed to investigate the role of Ser-263 in NH_3 translocation.

Simulations

MD simulations were carried out with the GROMACS package (17,18), using NPT and periodic boundary conditions. The GROMOS87 force field (19) was applied to the protein, and the parameters for the lipid were those used in previous MD studies of lipid bilayers (20–23). The charges of NH_3 and NH_4^+ were obtained by a restrained ESP-fit method using the ChelpG approach (24). The charge on the nitrogen of NH_3 is -1.077, and the charges on the hydrogen atoms are $+0.359$. In NH_4^+, the nitrogen charge is -0.824, and the hydrogen charges are $+0.456$. The linear constraint solver (LINCS) method (25) was used to constrain bond lengths, allowing an integration step of 2 fs. Electrostatic interactions were calculated with the particle mesh Ewald algorithm (26,27). A constant pressure of 1 bar was applied independently in *X*, *Y*, and *Z* directions of the whole system with a coupling constant of 1.0 ps (28). The systems were subjected to energy minimizations to remove unfavorable contacts. Water, lipids, NH_4^+, NH_3, and protein were coupled separately to a temperature bath at 323 K using a coupling time of 0.1 ps (28).

RESULTS

NH_3 conductance through the channel in the first protonation state of His-168-His-318

To study NH_3 translocation under the first protonation state of His-168-His-318, simulation A1 was carried out. All the NH_3 molecules that were initially located at Am2−Am4 sites (referred to as nha1, nha2, and nha3 hereafter) moved to the cytoplasmic pore exit (bottom) region of the channel within the simulation time of 1310 ps (Fig. 3). Four snapshots (Fig. 3 *C*) demonstrated clearly how the NH_3 molecules moved toward the cytoplasmic exit gate to the bottom of the channel. It was observed that hydrogen bonding between the NH_3 molecules and His-168 ceased after ~1310 ps (Fig. 3 *A*), with a concomitant increase in the number of hydrogen bonds formed between the NH_3 and Tyr-32 or His-318, especially after 1310 ps (Fig. 3 *B*). The N^{ε} of His-318 and hydroxyl of Tyr-32 could form hydrogen bonds with the NH_3 molecules, pulling the molecules to the bottom area of the channel. Thus, hydrogen bonding between N^{ε} of His-318 and hydroxyl of Tyr-32 provides the driving force for transport of NH_3 molecules through the hydrophobic central core to the bottom region of the channel.

Fig. 4 shows nha2 going into aqueous solution at ~1550 ps and is clearly the first NH_3 molecule leaving the channel. After passage of the NH_3 molecules to the bottom region of the channel at ~1300 ps, nha2 formed a hydrogen bond with the hydroxyl group of Ser-263 (Fig. 4). This hydrogen bond drew the ammonia close to the exit gate, thus allowing the formation of new hydrogen bonds between the NH_3 and water molecules in aqueous solution. The time-dependent hydrogen bonds formed between nha2 and the atoms inside the channel

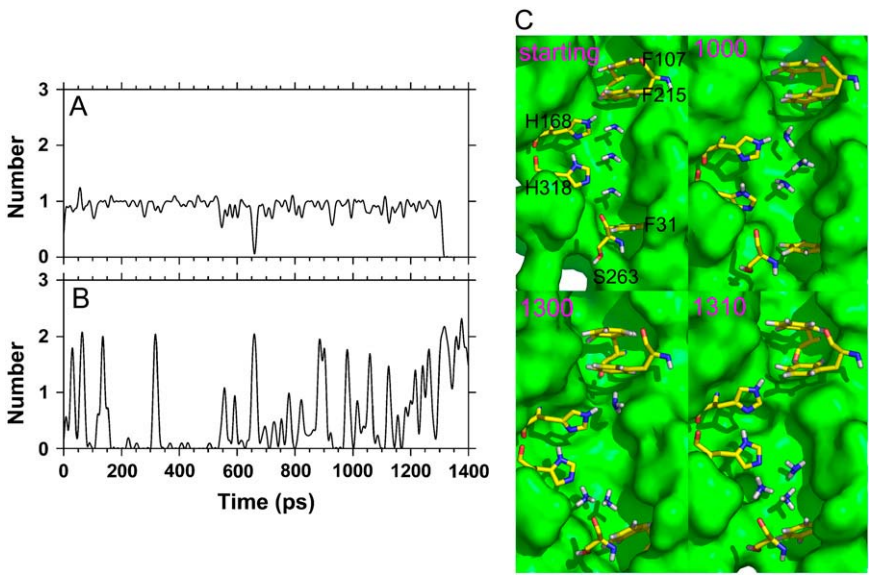

FIGURE 3 NH_3 molecules move to the bottom of the channel in trajectory A1. Numbers of the hydrogen bond between NH_3 molecules and His-168 (*A*) and between NH_3 molecules and His-318, Tyr-32 (*B*) versus time. Curves are obtained by 10 ps averaged. (*C*) Side views of the starting structure and three snapshot structures (1000, 1300, and 1310 ps). In side views, NH_3 molecules are drawn as white and blue sticks and water molecules are displayed as red and white sticks. F31, F107, H168, F215, S263, and H318 are displayed as colored sticks. The position of Y32 is indicated by an arrow.

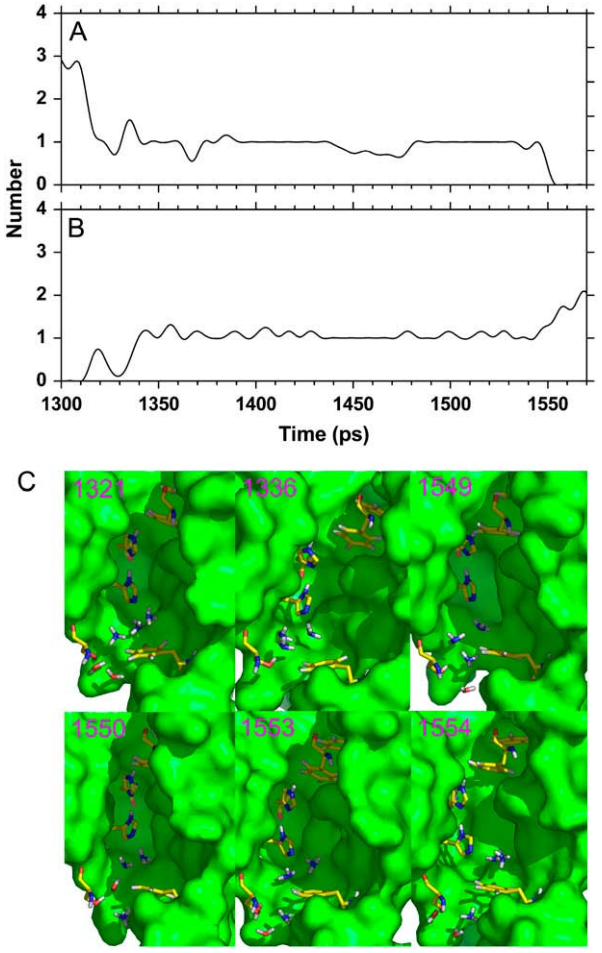

FIGURE 4 Process of the first NH_3 (nha2) leaving the channel in trajectory A1. Time-dependent hydrogen bonds between nha2 and the atoms inside the channel (including other NH_3 molecules, His-318 and Tyr-32) (*A*) and between nha2 and the atoms outside the channel (Ser-263 and water molecules) (*B*). Curves are obtained by 5 ps averaged. (*C*) Side views of six snapshot structures (1321, 1336, 1549, 1550, 1553, and 1554 ps, respectively). Hydroxyl of Ser-263 interacting with NH_3 through direct hydrogen bonding (1321, 1336, and 1549 ps) or water bridge (1550 ps).

(Fig. 4 *A*) and those between nha2 and the atoms outside the channel (Fig. 4 *B*) show that the number of internal hydrogen bonds decreased from ~1545 ps onward, whereas the external hydrogen bonds increased from ~1542 ps onward. Therefore, Ser-263 is deemed to be the key residue in NH_3 translocation through the channel. This residue acts as a pivoting arm, drawing the NH_3 molecule out of the channel. This result is consistent with a biological role for the conserved Ser-263 residue present in the transporter protein family. We postulated that Ser-263 plays an essential role in proteins belonging to the ammonium transporter family.

The exit processes of the other two NH_3 molecules in the channel are very similar to that of ammonia nha2 (Fig. S1, Supplementary Material). The hydroxyl of Ser-263 interacts with nha3 after the departure of nha2, pulling the NH_3 molecule out of the cytoplasmic exit pore and initiating the departure of the molecule nha3 from the channel at 1845 ps (Fig. S1A). The last NH_3 molecule (nha1) remained at the bottom of the channel by interactions primarily with Tyr-32 and His-318. In slight contrast with nha2 and nha3, nha1 interacts with Ser-263 via a water bridge (Fig. S1B). At ~5000 ps, nha1 exits the channel into the cytoplasm along with the water molecule.

Molecules nha1, nha2, and nha3 are initially located at Am2–Am4 sites, but they do not sequentially leave the channel in numerical order. Rather, nha2 is the first molecule that leaves the channel, followed by nha3, and finally by nha1. This is attributed to the random movement of these molecules while in the chamber, shifting forward and backward to varying degrees. They frequently change the relative order of their positions in the chamber of the channel, especially from 1000 ps onward.

Conducting NH_3 through the channel in the second state of His-168-His-318

In contrast to simulation A1, hydrogen atoms were added to the system His-168-His-318 in simulation A2 in accordance with the second protonation state explained earlier (Table 1 and Fig. 1 *C*). It took ~8 ns for the three NH_3 molecules to exit the channel. The NH_3 molecule nha2 exited the channel at ~500 ps (Fig. 5), followed by nha1 at ~850 ps (Fig. S2, Supplementary Material). Similar to trajectory A1, the hydroxyl groups of Ser-263 and water molecules were also found to play important roles in the translocation of the ammonia molecules through the channel in trajectory A2. But, in comparison with trajectory A1, the two ammonia molecules passed the channel much faster in trajectory A2.

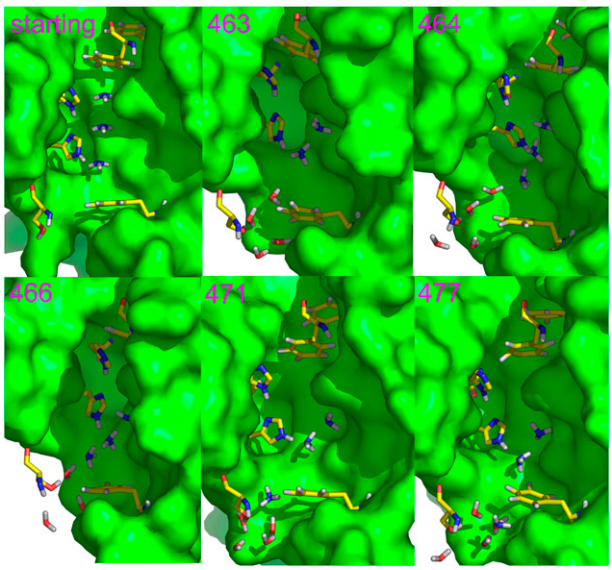

FIGURE 5 Process of the ammonia nha2 leaving the channel in trajectory A2. The starting structure and five snapshots (463, 464, 466, 471, and 477 ps) are shown.

This could be attributed to the strong hydrogen-bond network formed among the three NH_3 molecules and the $N^{\varepsilon}H$ of His-318 (Fig. 5). In other words, His-318 functions as a 'springboard' to facilitate the passage of the three ammonia molecules through the central core to the bottom area of the channel, thus allowing the ammonia molecules to interact with Ser-263. Hence, the consequent location of the NH_3 molecule near the cytoplasmic exit gate favors its departure from the channel into aqueous solution.

Interestingly, recurrence of the translocation process was also discovered during the simulation. For example, the molecule nha1, which had exited the channel at ~850 ps, was found in the channel again at ~1000 ps (Fig. S2). In addition, a water molecule was also found to have completely entered the channel at ~1310 ps. Thus, the simulation indicated that both water and NH_3 molecules could return to the bottom area of the channel, implying that the characteristic of the channel as a one-way valve to conduct NH_3 is not determined by the bottom exit gate but rather by the top entrance gate of the channel. Indeed, upward diffusion of NH_3 from the bottom region of the channel to the area above the His-168 residue was not observed during the whole simulation.

The ammonia molecule, nha3, also formed hydrogen bonds with Ser-263 and finally exited the channel at ~8100 ps (Fig. S3, Supplementary Material). Thereafter, the water molecule was found to leave the channel into the cytoplasm. The process by which the water molecule exited the hydrophobic channel was similar to the translocation process of NH_3. The conserved Ser-263 residue plays critical roles in these processes via hydrogen bonding with ammonia or water molecules.

Exit gating mechanism

At the cytoplasmic exit of the channel, two different conformational states, P63 (PDB: 1XQF) and R3 (PDB: 1XQE), have been observed in two different crystal forms (12). The distance between Phe-31 and Val-314 is ~8.0 Å in the P63 form and 10.5 Å in the R3 form. On the basis of these experimental results, it was postulated that the exit gating mechanism requires remarkable structural changes to the channel during NH_3 translocation (12,14) with a fluctuation distance between Phe-31 and Val-314 from 8.0 Å to 10.5 Å. To determine if this proposed exit gating mechanism is reasonable, the distance of Phe-31 to Val-314 was monitored along the simulation time in trajectory A1 (Fig. 6). We did not observe the expected large fluctuation in distance during the translocation of NH_3 through the channel. In fact, limited distance fluctuations (from 8.0 to 8.8 Å) were observed throughout the three periods coinciding with the exit of the three NH_3 molecules from the channel (Fig. 6). Therefore, the proposed exit gating mechanism requiring significant structural contortion of the channel might not exist. The same observations are also made in the simulation for trajectory 2.

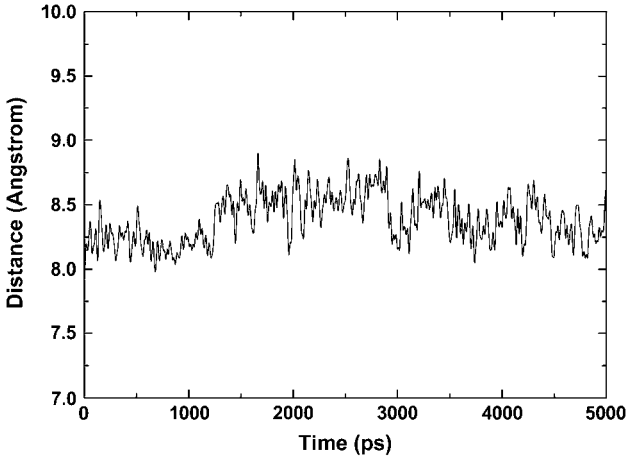

FIGURE 6 Distance between Phe-31 and Val-314 versus time in the processes of NH_3 molecules leaving in trajectory A1. Curve is obtained by 10 ps averaged.

It is reasonable to conclude, therefore, that marked conformational change is not essential for the passage of NH_3 through the channel.

Based on the above analyses of simulations A1 and A2, a new exit gating mechanism is proposed: NH_3 can move through the channel toward the cytoplasmic pore region and exit the channel into the cytoplasm via the exit gate formed by Phe-31, Ile-266, Val-314, and His-318. Hydrogen bonding is the most important driving force for the translocation of NH_3 molecules through the channel. His-318 serves as the springboard to facilitate the passage of the ammonia molecule toward the cytoplasmic end of the channel. In this process, significant conformational change of the channel is not essential. Instead, Ser-263 plays an essential role, acting as a pivoting arm to finally mediate the departure of NH_3 from the channel.

Role of Ser-263 in conducting NH_3

To illustrate the importance of Ser-263 in NH_3 translocation, simulation B was performed on a mutant of AmtB, in which Ser-263 was mutated to an alanine residue. Hydrogen atoms were added to His-168-His-318 in the first protonation state described earlier (Fig. 1 *B* and Table 1). In contrast with trajectory A1 whereby the three NH_3 molecules are shown to exit the channel in 5 ns, none of the NH_3 molecules was observed to leave the hydrophobic channel in the duration of the 20-ns simulation time in trajectory B. Fig. 7 depicts the snapshot at 20 ns from trajectory B. It is clear from the persistent presence of all three NH_3 molecules within the channel that the S263A mutation abrogated the function of Ser-263 in mediating the final departure of NH_3 into the cytoplasm. Taken together, our data confirm that Ser-263 plays a key role in the translocation of NH_3 molecules.

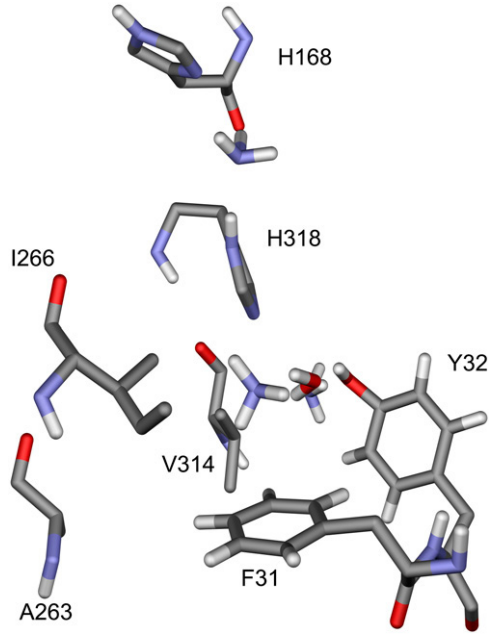

FIGURE 7 Snapshot at 20 ns from trajectory B. Ammonia molecules are shown as white and blue sticks.

Further analysis revealed that there are fewer water molecules around the exit gate in trajectory B than in trajectory A1. Because NH_3 is hydrophilic by nature, the predominantly more hydrophilic feature of trajectory A1 compared with trajectory B should provide a more conducive environment for the passage of NH_3 through the channel to the deep cytoplasmic bottom region and finally its departure through the exit pore into the essentially hydrophilic cytoplasm. On the other hand, the Ser-263–Ala mutation created a hydrophobic block by virtue of the aliphatic nature of alanine thereby effectively hindering the passage of hydrophilic NH_3 through the channel.

Fluctuation of entrance gate

It has been suggested that the perisplasmic entrance gate is formed by Phe-107 and Phe-215 (11,30). Analysis of the motions of these two residues in MD simulation, especially in conventional MD simulation, could provide useful information about the entry mechanism. Therefore, the distance between Phe-107 and Phe-215 against time in trajectory A1 was monitored (Fig. 8 *A*), and large fluctuations were observed ~2000–4000 ps. Upon further analysis, it was found that Phe-107 fluctuated on a large scale in the simulation (Fig. 8 *B*). Although Phe-215 does not show the large fluctuations seen in Phe-107, the aromatic ring of Phe-215 was observed to rotate ~360° during the simulation from 3100 to 3800 ps. Thus, the entrance gate could open spontaneously, and this mechanistic model is in contrast to the suggestion by Mo's group that NH_4^+ was responsible for opening the entrance gate via interaction with Phe-107 (30).

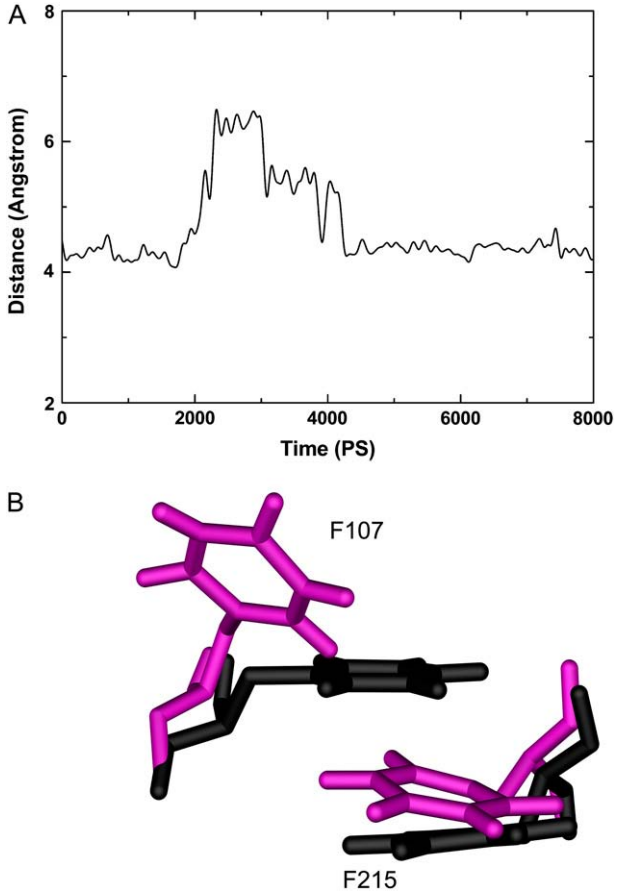

FIGURE 8 (*A*) Distance between two aromatic rings of Phe-107 and Phe-215 versus time. (*B*) The superposition of the starting structure (*black*) and the snapshot structure of 2500 ps (*cyan*) for Phe-107 and Phe-215.

MD simulation on the motion of NH_4^+ in the channel

It is noteworthy that although the simulations described so far have successfully elucidated the dynamic mechanism by which NH_3 molecules move through the hydrophobic channel into the aqueous cytoplasmic environment, the exact juncture where NH_4^+ releases its proton to form NH_3 remains a mystery. Does the NH_4^+ release its proton inside the channel? Our previous study using quantum chemistry methods reveals that proton transfer may take place between the imidazole ring of His-168 and NH_4^+ (29). To explore whether the NH_4^+ could enter freely into the channel to reach the His-168 residue, simulations were carried out to investigate the motions of the NH_4^+ molecule in the channel with the hydrogen atom added in the second protonation state described earlier. It was found that the NH_4^+ molecule did not enter the channel but exited the channel into the periplasm very rapidly (trajectory C1, Fig. 9 *A*), reaching the external Am1 site at ~1100 ps. Fig. 9 *A* shows that the distance of NH_4^+ from the starting position is time dependent, indicating that NH_4^+ resides over a longer period at the 3.3 Å and 7 Å positions

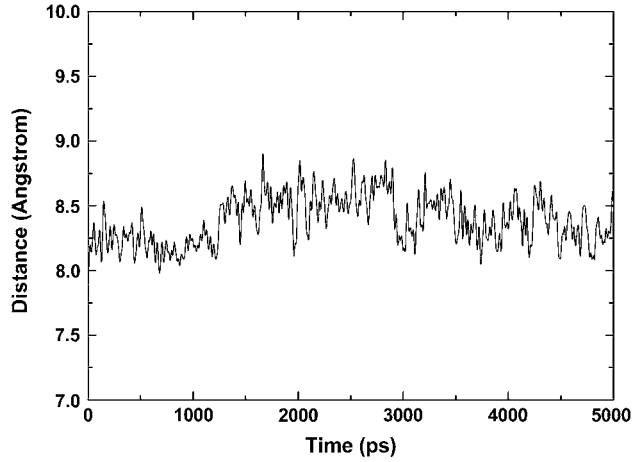

FIGURE 9 Time dependence of distance of NH_4^+ from the starting position in trajectory C1 (*A*) and C2 (*B*).

compared with other positions before its final escape from the channel. To validate this observation, one more simulation (trajectory C2 in Table 1) was performed on the same system but with different initial velocities assigned to each atom in the simulation (Fig. 9 *B*). Remarkably, trajectory C2 is very similar to trajectory C1, indicating that rapid entry of NH_4^+ into the periplasm through the entrance pore was not an incidental event. Therefore, deprotonation of the NH_4^+ at the periplasm is a critical prerequisite for its entry into the channel to reach the Am2 site. Recent work that supports this viewpoint was reported by Mo's group using steered molecular dynamics (SMD) simulations (30). They speculated that the deprotonation process occurs at the Am1 site with Asp-160 as the proton acceptor.

In simulation C2, NH_4^+ moves outward into the periplasm from the ~450-ps time point onward. Once the NH_4^+ reaches the external region, the molecule circulates around the Am1 site because of its interactions with Phe-107 and Trp-148 and Ser-219, suggesting that cation-π interaction is important for the process (Fig. S4, Supplementary Material). This postulation is in agreement with Liu's observations (13).

DISCUSSION

His-168-His-318 should adopt the first protonation state

Based on the results of our simulations, it is postulated that the first protonation state of the AmtB His-168-His-318 system (Fig. 1 *B*) is representative of the physiological status of this transporter protein, and this view is consistent with the observations of Khademi et al. First, our data on the fluctuation patterns of His-168-His-318 in trajectory A1 and A2 support this view. No significant structural changes to His-168 and His-318 in trajectory A1 (Fig. S5, Supplementary Material) were observed, and this is consistent with the known stability of His-168-His-318 in crystal structures. On the other hand, the His-168-His-318 in trajectory A2 showed very large-scale fluctuations that were incompatible with the B-factor in crystal structures (Fig. S5). Hence, the implication is that the structure of His-168-His-318 in the crystal form was abolished in trajectory A2. Second, the phenomena of water entering the pocket in trajectory A1 again suggest that the protein adopts the first protonation state of the His-168-His-318 system. Unlike the previously reported non-adiabatic molecular dynamics simulation (11), one water molecule was found to enter and remain inside the deep pocket of the channel via the exit pore after the departure of three ammonia molecules from the channel (Fig. 1 *A*, and Fig. S6 of Supplementary Material). Another water molecule dynamically entered and exited this pocket region via the exit pore. The water molecule(s) interacted with the N^{ε} of His-318 and hydroxyl of Tyr-32 to form hydrogen bonds. Indeed, a crystal structure of AmtB (PDB: 1XQF) shows that there is a water molecule in the pocket, whereas another crystal (PDB: 1XQE) demonstrates that there are two water molecules in the pocket, suggesting that our simulation results are in good agreement with the experimental results. However, no similar phenomenon was observed through trajectory 2, again implying that the physiologically relevant protonation state of His-168-His-318 adopted by the protein involves the addition of hydrogen atoms to N^{ε} of His-168 and N^{δ} of His-318, and this view is well supported by the work of Khademi et al.

Ser-263 functions like a 'pivoting arm' in NH_3 conductance

Simulation results indicate that NH_3 molecules leave the channel with the aid of Ser-263 through hydrogen-bond formation that drives the movement of NH_3 downward to the exit region. Subsequently, water molecules in the vicinity of the exit region form further hydrogen bonds to draw the NH_3 completely out of the channel. Further compelling evidence for this mechanism is that the substitution of Ser-263 by alanine abolishes the departure of NH_3 from the channel in trajectory B. The implication is that the residue Ser-263 functions like a 'pivoting arm' to shunt NH_3 into the cytoplasm.

Deduced mechanism of conductance

On the basis of SMD (30) and MD simulations, it was deduced that NH_4^+ releases a proton in the periplasm and reaches the Am2 site as NH_3. Mo et al. surmised that the deprotonation process occurs at the Am1 site with Asp-160 as the proton acceptor (30). We showed strong evidence that there is no obligatory requirement for NH_4^+ for the entrance gate to attain the open state. In addition, we found that the ammonia molecule is conveyed to the central region of the channel via a hydrogen-bond network involving His-168, His-318, Tyr-31, and the NH_3 molecule itself. Finally, the NH_3 exits the channel mediated by Ser-263 and water molecules present in the vicinity. Fig. 10 depicts the proposed

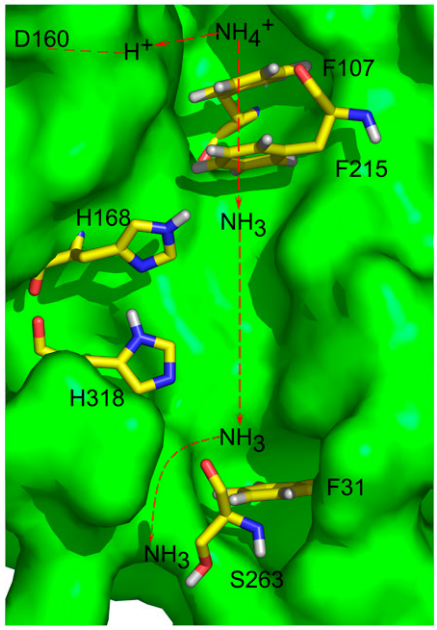

FIGURE 10 Deduced mechanism of the conductance of NH_3. Ammonium releases its proton at Am1 site. The ammonia moves to the bottom region of the channel with the help of the interactions from Tyr-31 and His-318. Finally, the hydroxyl of Ser-263 forms a hydrogen bond with NH_3, to pull the NH_3 from the bottom region of the channel into the cytoplasm.

translocation pathway of NH_3 through AmtB. However, more quantum mechanics-based simulations are required to resolve at the atomic level the deprotonation process by which an NH_4^+ molecule converts into NH_3 during translocation across the channel.

SUPPLEMENTARY MATERIAL

An online supplement to this article can be found by visiting BJ Online at http://www.biophysj.org.

The authors thank Dr Oi Wah Liew of Singapore Polytechnic for her help in preparing this manuscript.

This work was supported by grants from the State Key Program of Basic Research of China (2004CB518901), the State Key Program of R&D (2005BA711A04), and the Shanghai Key Basic R&D Program (grants 03DZ19228 and 05JC14092).

REFERENCES

1. Broach, J., C. Neumann, and S. Kustu. 1976. Mutant strains (nit) of *Salmonella typhimurium* with a pleiotropic defect in nitrogen metabolism. *J. Bacteriol.* 128:86–98.
2. Javelle, A., E. Severi, J. Thornton, and M. Merrick. 2004. Ammonium sensing in *Escherichia coli*. Role of the ammonium transporter AmtB and AmtB-GlnK complex formation. *J. Biol. Chem.* 297:8530–8538.
3. Marini, A. M., S. Vissers, A. Urrestarazu, and B. Andre. 1994. Cloning and expression of the MEP1 gene encoding an ammonium transporter in *Saccharomyces cerevisiae*. *EMBO J.* 13:3456–3463.
4. Ninnemann, O., J. C. Jauniaux, and W. B. Frommer. 1994. Identification of a high affinity NH_4^+ transporter from plants. *EMBO J.* 13: 3464–3471.
5. Marini, A. M., S. Soussi-Boudekou, S. Vissers, and B. Andre. 1997. A family of ammonium transporters in *Saccharomyces cerevisiae*. *Mol. Cell. Biol.* 17:4282–4293.
6. Drepper, T., S. Gross, A. F. Yakunin, P. C. Hallenbeck, B. Masepohl, and W. Klipp. 2003. Role of GlnB and GlnK in ammonium control of both nitrogenase systems in the phototrophic bacterium *Rhodobacter capsulatus*. *Microbiology.* 149:2203–2212.
7. Javelle, A., and M. Merrick. 2005. Complex formation between AmtB and GlnK: an ancestral role in prokaryotic nitrogen control. *Biochem. Soc. Trans.* 33:170–172.
8. Soupene, E., L. He, D. Yan, and S. Kustu. 1998. Ammonia acquisition in enteric bacteria: physiological role of the ammonium/methylammonium transport B (AmtB) protein. *Proc. Natl. Acad. Sci. USA.* 95: 7030–7034.
9. Soupene, E., H. Lee, and S. Kustu. 2002. Ammonium/methylammonium transport (Amt) proteins facilitate diffusion of NH_3 bidirectionally. *Proc. Natl. Acad. Sci. USA.* 99:3926–3931.
10. Meier-Wagner, J., L. Nolden, M. Jakoby, R. Siewe, R. Kramer, and A. Burkovski. 2001. Multiplicity of ammonium uptake systems in *Corynebacterium glutamicum*: role of Amt and AmtB. *Microbiology.* 174:135–143.
11. Khademi, S., J. O'Connell 3rd, J. Remis, Y. Robles-Colmenares, L. J. Miercke, and R. M. Stroud. 2004. Mechanism of ammonia transport by Amt/MEP/Rh: structure of AmtB at 1.35 Å. *Science.* 305:1587–1594.
12. Zheng, L., D. Kostrewa, S. Berneche, F. K. Winkler, and X. D. Li. 2004. The mechanism of ammonia transport based on the crystal structure of AmtB of *Escherichia coli*. *Proc. Natl. Acad. Sci. USA.* 101: 17090–17095.
13. Liu, Y., and X. Hu. 2006. Molecular determinants for binding of ammonium ion in the ammonia transporter AmtB-A quantum chemical analysis. *J. Phys. Chem. A.* 110:1375–1381.
14. Andrade, S. L. A., A. Dickmanns, R. Ficner, and O. Einsle. 2005. Crystal structure of the archaeal ammonium transporter Amt-1 from Archaeoglobus fulgidus. *Proc. Natl. Acad. Sci. USA.* 102:14994–14999.
15. de Groot, B. L., and H. Grubmuller. 2001. Water permeation across biological membranes: mechanism and dynamics of aquaporin-1 and GlpF. *Science.* 294:2353–2357.
16. Berendsen, H. J. C., J. P. M. Postma, W. F. van Gunsteren, and J. Hermans. 1981. Interaction models for water in relation to protein hydration. *In* Intermolecular Force. B. Pullman, editor. Reidel, Dordrecht, The Netherlands. 331–342.
17. Berendsen, H. J. C., D. van der Spoel, and R. van Drunen. 1995. GROMACS: a message-passing parallel molecular dynamics implementation. *Comput. Phys. Commun.* 91:43–56.
18. Lindahl, E., B. Hess, and D. van der Spoel. 2001. GROMACS 3.0: a package for molecular simulation and trajectory analysis. *J. Mol. Model. (Online).* 7:306–317.
19. van Gunsteren, W. F., and H. J. C. Berendsen. 1987. Gromos87 Manual. Biomos, Groningen, The Netherlands.
20. Berger, O., O. Edholm, and F. Jahnig. 1997. Molecular dynamics simulations of a fluid bilayer of dipalmitoylphosphatidylcholine at full hydration, constant pressure, and constant temperature. *Biophys. J.* 72: 2002–2013.
21. Marrink, S. J., O. Berger, P. Tieleman, and F. Jahnig. 1998. Adhesion forces of lipids in a phospholipid membrane studied by molecular dynamics simulations. *Biophys. J.* 74:931–943.
22. Tieleman, D. P., M. S. P. Sansom, and H. J. C. Berendsen. 1999. Alamethicin helices in a bilayer and in solution: molecular dynamics simulations. *Biophys. J.* 76:40–49.
23. Tieleman, D. P., H. J. C. Berendsen, and M. S. P. Sansom. 1999. An alamethicin channel in a lipid bilayer: molecular dynamics simulations. *Biophys. J.* 76:1757–1769.
24. Breneman, C. M., and K. B. Wiberg. 1990. Determining atom-centered monopoles from molecular electrostatic potentials. The need for high sampling density in formamide conformational analysis. *J. Comp. Chem.* 11:361–373.

25. Hess, B., H. Bekker, H. J. C. Berendsen, and J. G. E. M. Fraaije. 1997. LINCS: a linear constraint solver for molecular simulations. *J. Comp. Chem.* 18:1463–1472.

26. Darden, T. A., D. M. York, and L. G. Pedersen. 1993. Particle mesh Ewald: an N·log(N) method for Ewald sums in large systems. *J. Chem. Phys.* 98:10089–10092.

27. Essmann, U., L. Perera, M. L. Berkowitz, T. Darden, H. Lee, and L. G. Pedersen. 1995. A smooth particle mesh Ewald method. *J. Chem. Phys.* 103:8577–8592.

28. Berendsen, H. J. C., J. P. M. Postma, W. F. van Gunsteren, A. DiNola, and J. R. Haak. 1984. Molecular dynamics with coupling to an external bath. *J. Chem. Phys.* 81:3684–3690.

29. Zhu, W. L., X. J. Tan, C. M. Puah, J. D. Gu, H. L. Jiang, K. X. Chen, C. Felder, C. I. Silman, and J. L. Sussman. 2000. How does ammonium interact with aromatic groups? A density functional theory (DFT/B3LYP) investigation. *J. Phys. Chem. A.* 104:9573–9580.

30. Lin, Y. C., Z. X. Cao, and Y. R. Mo. 2006. Molecular dynamics simulations on the *Escherichia coli* ammonia channel protein AmtB: mechanism of ammonia/ammonium transport. *J. Am. Chem. Soc.* 128:10876–10884.